

Letter to Neuroscience

EVIDENCE FOR AN EPHAPTIC FEEDBACK IN CORTICAL SYNAPSES: POSTSYNAPTIC HYPERPOLARIZATION ALTERS THE NUMBER OF RESPONSE FAILURES AND QUANTAL CONTENT

L. L. VORONIN,*† M. VOLGUSHEV,‡§|| M. SOKOLOV,* A. KASYANOV,§¶
M. CHISTIAKOVA,‡§|| and K. G. REYMAN¶

*Brain Research Institute, Russian Academy of Medical Sciences, per. Obukha 5, 103064 Moscow, Russia

‡Max Planck Institute for Brain Research, Deuschordenstrasse 46, 60528 Frankfurt/Main, Germany

§Institute of Higher Nervous Activity and Neurophysiology, Russian Academy of Sciences, 5a Butlerova Street, 117485 Moscow, Russia

||Department of Neurophysiology, Ruhr-University Bochum, 44801 Bochum, Germany

¶Leibniz Institute for Neurobiology, Brennekestrasse 6, 39008 Magdeburg, Germany

Key words: synaptic transmission, ephaptic feedback, visual cortex, hippocampus, CA1, rat.

The amplitude of excitatory postsynaptic potentials and currents increases with membrane potential hyperpolarization. This has been attributed to an increase in the driving force when the membrane potential deviates from the equilibrium potential of the respective ions.¹⁷ Here we report that in a subset of neocortical and hippocampal synapses, postsynaptic hyperpolarization affects traditional measures of transmitter release: the number of failures, coefficient of variation of response amplitudes, and quantal content, suggesting increased pre-synaptic release. The result is compatible with the hypothesis of Byzov^{4,5} on the existence of electrical (or “ephaptic”¹⁵) linking in purely chemical synapses. The linking, although negligible at neuromuscular junctions,^{17,27} could be functionally significant in influencing transmitter release at synapses with high resistance along the synaptic cleft.^{5,33} Our

findings necessitate reconsideration of classical amplitude–voltage relations for such synapses. Thus, synaptic strength may be enhanced by hyperpolarization of the postsynaptic membrane potential. The positive ephaptic feedback could account for “all-or-none” excitatory postsynaptic potentials at some cortical synapses,^{25,30} large evoked⁷ and spontaneous¹⁸ multiquantal events and a high efficacy of large “perforated” synapses whose number increases following behavioural learning⁶ or the induction of long-term potentiation.^{9,12} © 1999 IBRO. Published by Elsevier Science Ltd.

We tested a corollary of the hypothesis^{4,5} on intrasynaptic positive feedback due to the current dividing between the synaptic cleft and presynaptic ending. The electrical scheme described elsewhere^{5,33} shows that when the cleft resistance is large enough, excitatory postsynaptic current (EPSC) branch passing through the presynapse can induce a significant depolarization and increase transmitter release. The same effect is expected from artificial intracellular hyperpolarizing currents.²⁷

To test this prediction, we studied minimal EPSCs recorded from rat visual cortex (Fig. 1a,b). As expected,¹⁷ EPSC amplitudes increased during somatic hyperpolarization (Fig. 1d). However, Fig. 1d–g shows that the increase was partially due to reduction of the number of response failures (N_0) estimated by two methods (see Fig. 1 legend). Another input showed no N_0 changes (Fig. 1c) rejecting explanations based on general postsynaptic alterations. Significant ($P < 0.03$) N_0 decreases were

†To whom correspondence should be addressed.

Abbreviations: AMPA, α -amino-3-hydroxy-5-methyl-4-isoxazolepropionate; AMPAR, AMPA-type glutamate receptor; AP5, d-2-amino-5-phosphonopentanoate; A–V relation, amplitude–voltage relation; CNQX, 6-cyano-7-nitroquinoxaline-2,3-dione; CV, coefficient of variation of response amplitude; E , mean response amplitude; EGTA, ethyleneglycolbis(aminoethyl-ether)tetra-acetate; EPSC, excitatory postsynaptic current; EPSC1/2, EPSC induced by the first/second pulse; EPSP, excitatory postsynaptic potential; GluR, glutamate receptor; HEPES, N-2-hydroxyethyl-piperazine-N'-2-ethanesulphonic acid; LTP, long-term potentiation; m , mean quantal content; mGluR, metabotropic glutamate receptor; MP, membrane potential; N_0 , number of response failures; NMDA, N-methyl-d-aspartate; NMDAR, NMDA-type glutamate receptor; r , coefficient of correlation; S_n , standard deviation of the noise; v , quantal size.

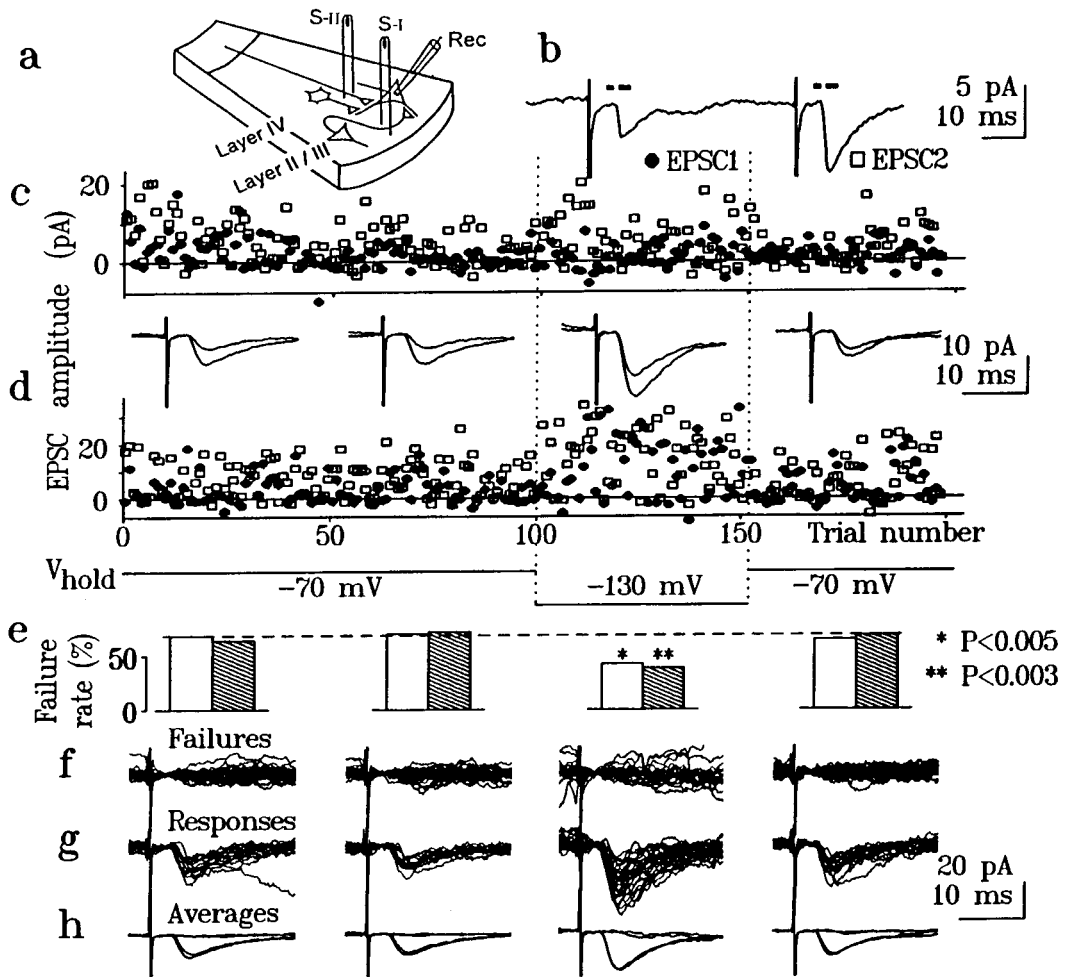


Fig. 1. Failure rate reduction during hyperpolarization of a visual cortex neuron. (a) Arrangement of stimulating (S-I, S-II) and recording (Rec) electrodes in the cortical slice. (b) Averaged ($n = 100$) EPSC1 and EPSC2 induced by the first and second paired S-I stimulations, respectively. Bars indicate windows for amplitude measurements. (c, d) Single EPSC1 (dots) and EPSC2 (squares) amplitudes for S-I (c) and S-II (d) inputs and averaged ($n = 50$) EPSC1 and EPSC2 (d). (e) Failure rates for EPSC1 (S-II input) determined by visual selecting failures and doubling the number of negative amplitudes (open and hatched columns). Asterisks mark significant differences as compared to -70 mV. (f, g) All EPSC1 failures (f) and successes (g) from the respective parts of the experiment. (h) Respective averages for EPSC1 and EPSC2. Note the absence of paired-pulse facilitation of successes (h) but a strong facilitation of the response included failures (d). Voltage-clamp whole cell recordings were made from slices of visual cortex of four- to six-week-old rats (Albino, MPI for Brain Research, Frankfurt).³⁰ The slices were superfused with solution containing (in mM): NaCl 125, KCl 2.5, CaCl₂ 2, MgCl₂ 1, NaH₂PO₄ 1.25, NaHCO₃ 25, d-glucose 10, l-Glutamine 0.5 bubbled with 95% O₂ and 5% CO₂ at 30°C. Bicuculline methiodide (0.35–0.5 μ M) or picrotoxin (100 μ M, Sigma) were added in half of the experiments. No GABA antagonists were present in the other visual cortex experiments (as in Fig. 3Aa). The recording pipette contained (in mM): Cs-methanesulphonate or K-gluconate 127, KCl 20, MgCl₂ 2, Na₂ATP 2, HEPES 10, EGTA 1 (resistance of 2–6 M Ω). Paired (50 ms) stimuli (1–10 V, 0.04–0.1 ms) were applied every 8–20 s through bipolar tungsten electrodes positioned in layers I–II and IV (Fig. 1a, S-I and S-II). Stimuli were adjusted to induce minimal EPSCs with response failures. The serial resistance was monitored with small voltage steps. Different holding MPs were applied either continuously for 20–150 trials or with alterations after every one or 10 trials. Mostly “resting” (-70 mV) and hyperpolarizing (-100 to -130 mV) MPs were used. We used MPs > -40 mV predominantly at the end of the experiments because they often induced LTP even under voltage clamp. Data were digitized at 5 or 10 kHz. Amplitudes were measured as the difference between average currents in two windows of 1–4 ms width (b, bars) so that the mean EPSC amplitudes were positive. The number of failures (N_0) was estimated using two methods.³² Firstly, we separated failures and successes visually (f,g). Consideration of superimposed successes and averaged failures (g,h) was used to control the separation. Secondly, we estimated N_0 as double number of negative amplitudes. The similarity (e) and high correlation between N_0 estimated by the two methods ($r = 0.97$, $n = 52$, $P < 0.0001$) confirmed the adequacy of the visual selection. The failure rates (N_0/n) were presented either as absolute ratios (e) or as a percentage of their logarithm at hyperpolarizing MPs relative to that at resting MPs. The statistical significance of N_0 changes was assessed applying Chi-square test. Only inputs with $N_0 > 2$ before hyperpolarization and with summary $n > 50$ (up to 199) were used in the neocortical experiments. $P < 0.03$ was taken as “statistically significant” if not otherwise specified. There were no significant differences for experiments with different inputs, protocols of current injections and micropipette solutions. Therefore, the results are described together. There were also no differences for experiments with GABA_A antagonists present (Fig. 1) or absent (Fig. 3Aa) after exclusion of three EPSCs with outward currents at 0 MP recorded in two experiments without GABA_A antagonists.

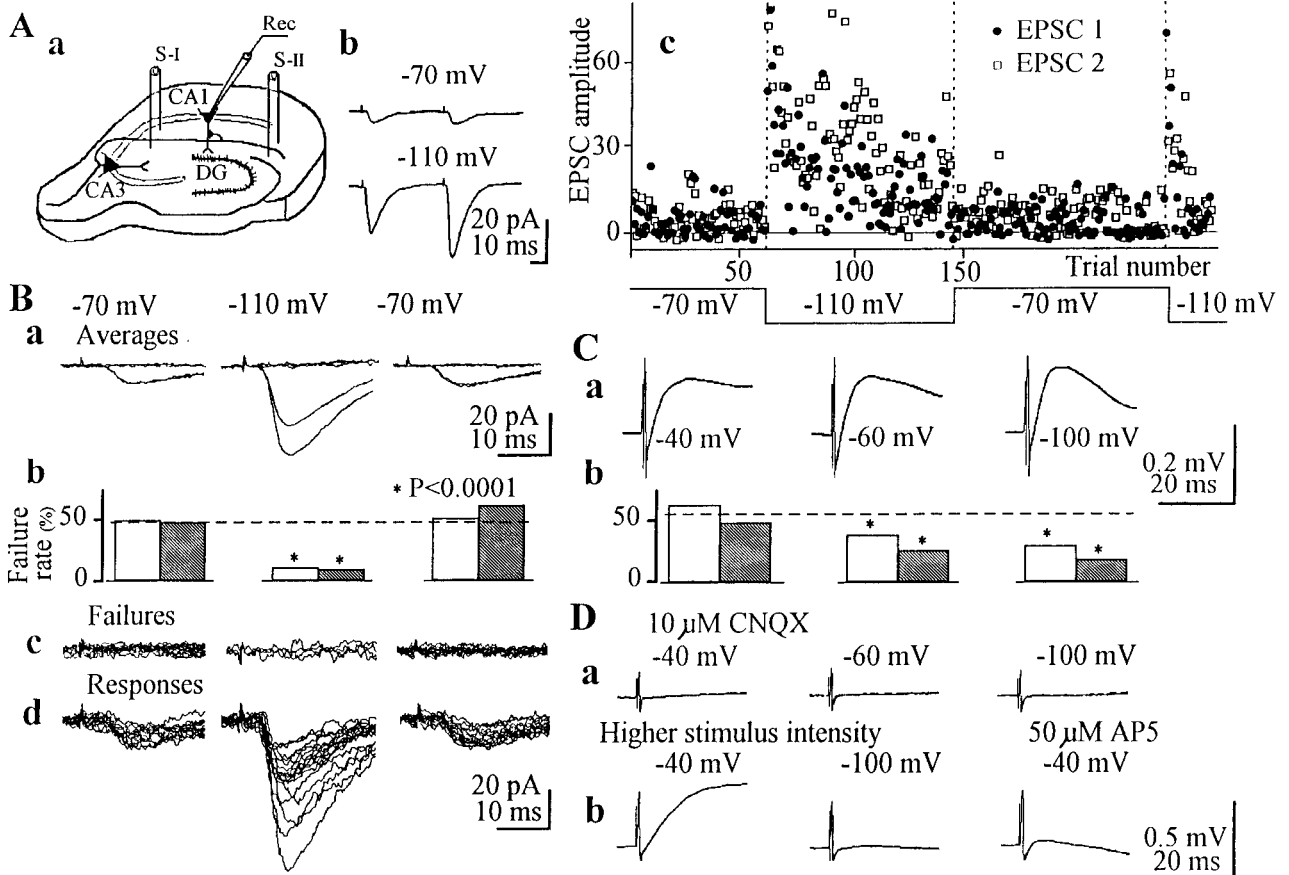


Fig. 2. Effects of hyperpolarization and pharmacological treatments on hippocampal responses. (Aa) Electrode arrangement. (Ab) Averaged EPSCs. (Ac) Single EPSC amplitudes at different MPs. (B) Same neuron; averages (a) and failure analysis (b–d) analogous to Fig. 1e–h. (Ca) Averaged ($n = 160$) EPSPs of another neuron. (Cb) Same as in Bb. (Da) Suppression of EPSPs in the same neuron by CNQX. (Db) Appearance of a response to a larger stimulus current ($\times 1.5$) at -40 mV and its suppression by hyperpolarization and by AP5. Averages ($n = 20$ – 40) are shown. The hippocampal experiments were performed on Wistar rats bred at the Leibniz Institute of Neurobiology, Magdeburg and Brain Research Institute, Moscow. The methods^{1,24} were similar to those described in Fig. 1. However, the perfusion solution was slightly different (NaCl 124, KCl 1.5, CaCl₂ 2.45, MgCl₂ 1.3, KH₂PO₄ 1.25, NaHCO₃ 25, d-glucose 10) and picrotoxin (100 μ M) was always used. Tetrodotoxin (Affinity Research Products, 2 nM) was added to avoid the epileptic activity. Both voltage ($n = 9$ EPSCs) and current clamp modes ($n = 20$ EPSPs) were employed using K-gluconate electrodes. CNQX (10 μ M, Tocris) were used to block AMPARs, and AP5 (50 μ M, Cambridge Research Biochemicals) to block NMDARs.

found in 7/23 inputs (5/14 neurons, see Fig. 3Ba, dashed columns).

To examine whether such changes exist in other structures and under different recording conditions, we studied excitatory postsynaptic potentials (EPSPs; Fig. 2Ca) and EPSCs (Fig. 2Ab) in the hippocampus (Fig. 2Aa). Hyperpolarization led to significant ($P < 0.03$) N_0 decreases (Fig. 2Ac, B, Cb) in 10/29 inputs (9/18 neurons; Fig. 3Ba, open columns).

Figure 2Ca shows that the averaged EPSP amplitudes changed only slightly with hyperpolarization in spite of N_0 changes (Fig. 2Cb). This is due to a decrease in the amplitude of successes with hyperpolarization (14/20 current clamp recordings), explained by the anomalous rectification¹³ and reduced activation of voltage-dependent channels²⁶. Changes in monosynaptic *N*-methyl-d-aspartate

(NMDA) receptor (NMDAR)-mediated components⁸ should be of lesser importance because the hippocampal EPSPs were suppressed by antagonists of α -amino-3-hydroxy-5-methyl-4-isoxazolepropionate (AMPA) receptors (AMPA) receptors (AMPA) ($n = 6$ experiments; Fig. 2Da). Slower responses could be induced under AMPARs blockade after significant (1.4–2 times) increases in the stimulus strength (Fig. 2Db). They were blocked by hyperpolarization ($n = 6$) or by d-2-amino-phosphonopentanoate (AP5) (Fig. 2Db; $n = 5$) suggesting their mediation by NMDARs. Therefore, the minimal responses at the -40 to -130 mV membrane potentials (MPs) were almost completely mediated by AMPARs.

The N_0 reduction suggests presynaptic changes. To test this further, we determined the coefficient of variation of response amplitude (CV) and mean quantal content (m) which are traditional measures

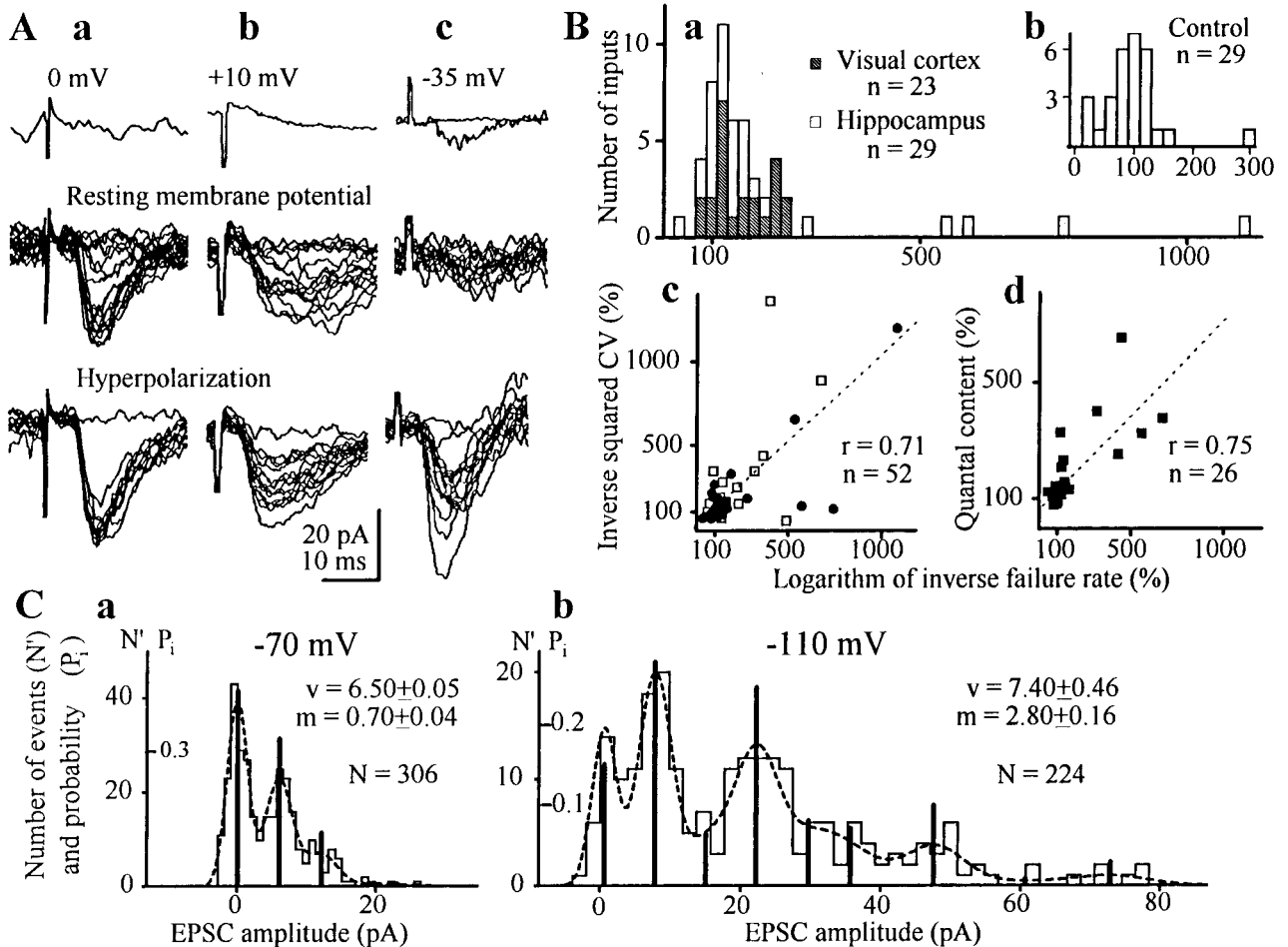


Fig. 3. Variance and quantal analysis of hyperpolarization effects. (A) Visual cortex (a) and hippocampal (b, c) EPSCs at various MPs. Averages during depolarization (upper row in a–c, $n = 10$, 100 and 97, respectively) show the absence of outward (inhibitory) currents. In c, all successes ($n = 3$) were also averaged. (B) Summary of changes in N_0 (a), CV^{-2} (c) and m (d). (b) Control series without hyperpolarization of hippocampal neurons. The control does not differ from a Gaussian ($P > 0.2$) indicating only small spontaneous trends (mainly N_0 increases). In contrast, the experimental distribution (a, open columns) is significantly different from a Gaussian ($P < 0.01$, Kolmogorov–Smirnov test) and control ($P < 0.001$). Dots, open and closed squares represent data for EPSC1, EPSC2 and pooled data,¹⁹ respectively. Dashed lines represent linear regressions ($P < 0.001$ for both correlation coefficients, r). (C) Deconvolution analysis (EPSCs from Fig. 2B). Columns and dashed curves represent experimental and predictive distributions, respectively (number of events, N'). Bar heights (probabilities, P_i) give deconvolution solutions. Insets give quantal size (v) and m (\pm S.E.M.). Noise standard deviation $S_n = 1.5$ pA. CV^{-2} was corrected for the noise variance and for the amplitude linear regression when it was statistically significant ($P < 0.05$). To determine m , we used an “unconstrained” noise deconvolution.¹ The algorithm searched for discrete distributions (C, bars) with coordinates x_i (distance from 0) and P_i (heights). The weighted mean interval between the bars was used to define quantal size (v) and m ; 0.2 v was taken as intrinsic quantal variance.¹ Because stimuli had to be applied at a low rate (about 0.1 Hz) to diminish amplitude depression, samples were small (120 to 516; 234 ± 11 , mean \pm S.E.M., $n = 52$ distributions) even when we combined EPSC1 and EPSC2 measurements¹⁹. Even at these testing intervals the low-frequency depression³² was sometimes evident especially during hyperpolarization (Fig. 2Ac). Computer simulations¹ show that at $n = 200$, reliable estimates are obtained provided $v/S_n > 2.5$. The mean v/S_n was 3.7 ± 0.2 ($n = 52$). Similar m for cases without significant changes in N_0 (Fig. 3Bb, cloud around 100%; Fig. 4c,d), correlations between m and CV^{-2} ($r = 0.67$, $n = 52$, $P < 0.0001$) and especially between v determined by the spectral analysis³² and our computer algorithm ($r = 0.86$, $n = 52$, $P < 0.0001$) confirm the adequacy of the latter and of the suggested small intrinsic quantal variance.

of transmitter release.^{17,32} In addition to decreasing N_0 , hyperpolarization caused the disappearance of small responses (Fig. 3Aa) and moderate (Fig. 3Aa,b) or large (Fig. 3Ac) increases in the amplitude of the largest responses. Responses (Fig. 3Aa) then

resembled “synchronized” all-or-none responses with low variances.^{25,30} Accordingly, CV^{-2} and m increased (Fig. 3Bc,d, C) when hyperpolarization was effective in reducing N_0 . These alterations are compatible with presynaptic changes (but see Ref.

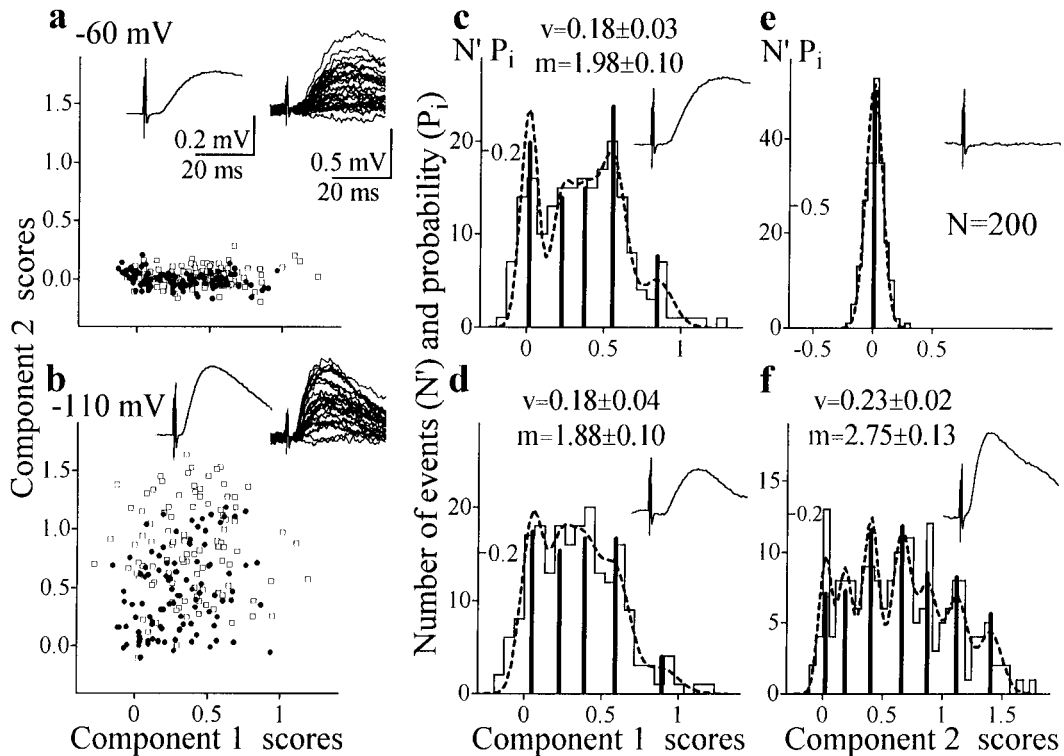


Fig. 4. Component analysis of a hippocampal EPSP with an apparent latency decrease during hyperpolarization. (a,b) Plots of component scores. (c–f) Amplitude distributions for components 1 (c, d) and 2 (e, f). The dashed curve in e represents the noise distribution. See Fig. 3C for other notations. Insets show averaged ($n = 100$) and 30 consecutive single EPSPs (a,b) and averaged isolated components (c–f, $n = 65, 15, 35$ and 17, respectively). For all distributions, $n = 200$. $S_p = 0.051, 0.075, 0.060, 0.067$ for c–f, respectively. To improve the signal-to-noise ratio in the hippocampal experiments, we used a covariance measure provided by the principal component analysis.² Scores of the first principal component were determined from the initial slope and the peak. Such integral “covariance amplitudes” were strongly correlated with more common measures of peak amplitudes. They were normalized to pA or mV and referred as “amplitudes” for simplicity. The noise was measured for a window of the same duration (5–14 ms) but before stimulus. To identify the response components (c–f, insets) we used a procedure described elsewhere.² In brief, we averaged responses corresponding to positive values of one component and about 0 values of another component. For example, to identify component 1 (d, inset) we averaged responses corresponding to the dots around zero y-values (b). Note a faster kinetics of the new component suggesting a proximal location of the respective synapses. The appearance of the new components explains occasional lack of expected reduction in the paired-pulse facilitation during hyperpolarization (Fig. 2Ba, but see Fig. 1d where such a reduction is evident).

10). It should also be noted that peak variations in Fig. 3Cb did not fit a binomial model also suggesting release synchronization.^{1,30}

In four hippocampal neurons, the MP hyperpolarization was associated with latency decreases of 1.6–2 ms (Figs 2Ba, 4a,b, insets). The latency decrease³⁴ could be due to the activation of pre-synaptically^{2,28,31,32} or postsynaptically “silent”¹⁴ synapses. We applied a novel procedure² and in all four EPSPs we found components which were not detected at the resting MP (“virtually silent” inputs). Figure 4a shows that only one component was present at -60 mV: component 2 scores did not differ from the background noise scores (Fig. 4e). During hyperpolarization, a short latency component 2 appeared (Fig. 4b, ordinate; 4f, inset). Since component 1 did not increase (Fig. 4c, d), both the amplitude increase and the latency decrease of the

averaged EPSP (Fig. 4a, b, insets) were due to the appearance of component 2 (Fig. 4f).

The changes in N_0 , CV and m could be due to several postsynaptic reasons. (1) Inhibitory responses could become depolarizing. We discard this possibility because in all hippocampal experiments GABA_A blockers were present. Moreover, depolarizing the cells to -35 to -45 mV or even zero or positive MP (Fig. 3A, altogether $n = 17$) did not reveal outward currents except in three visual cortex recordings which had been discarded (Fig. 1 legend). (2) Low amplitude (below noise level) responses could have increased due to the increased driving force and became measurable. However, the amplitude should have increased more than 10-fold (compare the average failures and the smallest responses, Fig. 1h,g) which is far above the value (less than twofold) predicted by the linear

amplitude–voltage (A–V) relation. Moreover, the classical relation does not explain the increases in the mean EPSC amplitudes (Figs 1, 2Ab), the latency decreases (Fig. 2Ba, 4a, b) and the appearance of new components (Fig. 4e, f). (3) Expression of new glutamate receptor (GluR) clusters. However, so far there is no evidence for such a mechanism in the numerous studies of the voltage dependences of AMPAR currents.¹⁶ (4) Up-regulation of “spare” receptors due to indirect current effects (such as changes in ionic concentration). In principle, GluRs are modulated by a number of agents.^{8,20} However, the related changes are expected to develop/recover with slow time-courses (see Ca²⁺ induced inactivation of NMDAR channels²⁰) and not to be strong enough to induce even the appearance of new components.

Therefore, we favour “presynaptic” explanations. One possibility is that changes in extracellular ionic concentration result in alterations of transmitter release. However, early results²⁷ suggest that the major effect of postsynaptic hyperpolarization is a reduced extracellular K⁺ associated with *m* reduction. The second possibility is the involvement of a retrograde messenger, as assumed in long-term potentiation (LTP) studies.³ However, the messengers are presumably released by postsynaptic depolarization. To fit our data, hyperpolarization should suppress the release of the messenger which at rest would inhibit transmitter release. A hypothetical possibility could be glutamate¹¹ acting on inhibitory presynaptic ionotropic²¹ or metabotropic²² GluRs (mGluRs). However, mGluR antagonists do not influence baseline hippocampal transmission²³ suggesting a lack of essential background glutamate release from postsynaptic neurons. Presynaptic cortical mGluR inhibition is potent mainly in young (one- to three-week-old) rats²² and following high-frequency stimulation.²³

Predominantly facilitatory after-effects of depolarizing pulses in CA1 neurons³³ are difficult to reconcile with this hypothesis.

The extracellular current could affect presynaptic release either directly or via glial cells.²⁹ We favour the former explanation because it is compatible with the ephaptic feedback hypothesis^{4,5,33} which allowed us to predict the described effects. This explanation is attractive because the positive feedback is also compatible with apparent release synchronization indicated by “all-or-none” responses^{25,30} and the appearance of large (“perforated”) synapses with invaginations (and therefore large cleft resistance^{5,33}) under conditions when synaptic efficacy is expected to increase.^{6,9,12}

Independent of its nature, the MP effect on release variables necessitates reconsideration of classical A–V relations which should be “supralinear” at hyperpolarizing MPs for some central synapses. The underlying mechanism may have important implications for controlling synaptic strength by the postsynaptic MP level and by currents from adjacent synapses. Our unpublished data indicate that adjacent excitatory synapses counterbalance postsynaptic hyperpolarization so that the A–V relations became linear for composite EPSCs even when some of the contributing synapses are endowed with the ephaptic feedback. Therefore, the feedback has a mechanism of self-limitation so that when numerous inputs are synchronously activated, abnormal boosting of large responses is prevented.

Acknowledgements—We thank Dr A. V. Astrelin for programming, Dr V. L. Ezrokhi for participation in a part of this work and Drs L. Bindman, A. L. Byzov, E. Cherubini, B. Katz, A. M. Kleschevnikov, A. Nistri and W. Singer for helpful comments. Supported by the Max-Planck Society, Volkswagen Foundation and Russian Foundation for Basic Research.

REFERENCES

1. Astrelin A. V., Sokolov M. V., Behnisch T., Reymann K. G. and Voronin L. L. (1997) Noise deconvolution based on L1-metrics and decomposition of discrete distributions of postsynaptic responses. *J. Neurosci. Meth.* **71**, 17–27.
2. Astrelin A. V., Sokolov M. V., Behnisch T., Reymann K. G. and Voronin L. L. (1998) Principal component analysis of minimal excitatory postsynaptic potentials. *J. Neurosci. Meth.* **79**, 169–186.
3. Bliss T. V. P. and Collingridge G. L. (1993) A synaptic model for memory: long-term potentiation in the hippocampus. *Nature* **361**, 31–39.
4. Byzov A. L. (1977) Model feedback mechanism between horizontal cells and photoreceptors of the vertebrate retina. *Neurophysiology* **9**, 89–94.
5. Byzov A. L. and Shura-Bura T. M. (1986) Electrical feedback mechanism in the processing of signals in the outer plexiform layer of the retina. *Vision Res.* **26**, 33–34.
6. Calverley R. K. S. and Jones D. G. (1990) Contributions of dendritic spines and perforated synapses to synaptic plasticity. *Brain Res. Rev.* **15**, 215–249.
7. Chuhma N. and Ohmori H. (1998) Postnatal development of phase-locked high-fidelity synaptic transmission in the medial nucleus of the trapezoid body of the rat. *J. Neurosci.* **18**, 512–520.
8. Collingridge G. L. and Singer W. (1990) Excitatory amino acid receptors and synaptic plasticity. *Trends Pharmac. Sci.* **11**, 290–296.
9. Edwards F. A. (1995) Anatomy and electrophysiology of fast central synapses lead to structural model for long-term potentiation. *Physiol. Rev.* **75**, 759–787.
10. Faber D. S. and Korn H. (1991) Application of the coefficient of variation methods for analyzing synaptic plasticity. *Biophys. J.* **60**, 1288–1294.
11. Glitsch M., Llano I. and Marty A. (1996) Glutamate as a candidate retrograde messenger at interneurone–Purkinje cell synapses of rat cerebellum. *J. Physiol., Lond.* **497**, 531–537.

12. Geinisman Y., de Toledo-Morell L., Morell F., Heller R. E., Rossi M. and Parshall R. F. (1993) Structural synaptic correlate of long-term potentiation: formation of axospinous synapses with multiple, completely partitioned transmission zones. *Hippocampus* **3**, 435–446.
13. Halliwell J. V. (1990) K⁺ channels in the central nervous system. In *Potassium Channels. Structure, Classification, Function and Therapeutic Potential*, pp. 348–381. Halsted, Ellis Horwood, Chichester, U.K.
14. Isaac J. T. R., Nicoll R. A. and Malenka R. C. (1995) Evidence for silent synapses: implications for the expression of LTP. *Neuron* **16**, 427–434.
15. Jefferys J. G. (1995) Nonsynaptic modulation of neuronal activity in the brain: electric currents and extracellular ions. *Physiol. Rev.* **75**, 689–723.
16. Jonas P. and Burnashev N. (1995) Molecular mechanisms controlling calcium entry through AMPA-type glutamate receptor channels. *Neuron* **15**, 987–990.
17. Katz B. (1969) *The Release of Neural Transmitter Substance*. Charles C. Thomas, Springfield, IL.
18. Korn H., Bausela F., Charpier S. and Faber D. S. (1993) Synaptic noise and multiquantal release at dendritic synapses. *J. Neurophysiol.* **70**, 1249–1254.
19. Kullmann D. M. and Nicoll R. A. (1992) Long-term potentiation is associated with increases in quantal content and quantal amplitude. *Nature* **357**, 240–244.
20. Legendre P., Rosemund C. and Westbrook G. L. (1993) Inactivation of NMDA channels in cultured hippocampal neurons by intracellular calcium. *J. Neurosci.* **13**, 674–684.
21. McGehee D. S. and Role L. W. (1996) Presynaptic ionotropic receptors. *Curr. Opin. Biol.* **6**, 342–349.
22. Sanchez-Prieto J., Budd D. C., Herrero L., Vazquez E. and Nicholls D. G. (1996) Presynaptic receptors and the control of glutamate exocytosis. *Trends Neurosci.* **19**, 235–239.
23. Scanziani M., Salin P. A., Vogt K. E., Malenka R. C. and Nicoll R. A. (1997) Use-dependent increases in glutamate concentration activate presynaptic metabotropic glutamate receptors. *Nature* **385**, 630–634.
24. Sokolov M. V., Rossokhin A. V., Behnisch T., Reymann K. G. and Voronin L. L. (1998) Interaction between paired-pulse facilitation and long-term potentiation of minimal EPSPs in rat hippocampal slices: a patch clamp study. *Neuroscience* **85**, 1–13.
25. Stratford K. J., Tarczy-Hornoch K., Martin K. A., Bannister N. J. and Jack J. J. B. (1996) Excitatory synaptic inputs to spiny stellate cells in cat visual cortex. *Nature* **382**, 258–262.
26. Stuart G. and Sakmann B. (1995) Amplification of EPSPs by axosomatic sodium channels in neocortical pyramidal neurons. *Neuron* **15**, 1065–1076.
27. Takeuchi A. and Takeuchi N. (1961) Changes in potassium concentration around motor nerve terminals, produced by current flow, and their effects on neuromuscular transmission. *J. Physiol., Lond.* **155**, 46–58.
28. Torii N., Tsumoto T., Uno L., Astrelin A. V. and Voronin L. L. (1997) Quantal analysis suggests presynaptic involvement in expression of neocortical short- and long-term depression. *Neuroscience* **79**, 317–321.
29. Vernadakis A. (1996) Glia-neuron intercommunications and synaptic plasticity. *Prog. Neurobiol.* **49**, 185–214.
30. Volgushev M., Voronin L. L., Chistiakova M., Artola A. and Singer W. (1995) All-or-none excitatory postsynaptic potentials in the rat visual cortex. *Eur. J. Neurosci.* **7**, 1751–1760.
31. Voronin L. L. (1983) Long-term potentiation in the hippocampus. *Neuroscience* **10**, 1051–1069.
32. Voronin L. L. (1993) On the quantal analysis of hippocampal long-term potentiation and related phenomena of synaptic plasticity. *Neuroscience* **56**, 275–304.
33. Voronin L., Byzov A., Kleschevnikov A., Kozhemyakin M., Kuhnt U. and Volgushev M. (1995) Neurophysiological analysis of long-term potentiation in mammalian brain. *Behav. Brain. Res.* **66**, 45–52.
34. Voronin L. L., Volgushev M., Chistiakova M., Kuhnt U. and Singer W. (1996) Involvement of silent synapses in the induction of LTP and LTD in hippocampal and neocortical neurons. *Neuroscience* **74**, 323–330.

(Accepted 16 March 1999)